



Cross-En-Route Aircraft Collision Risk Study Considering the Warning Adjustment Process

Fei LU¹

Original Scientific Paper Submitted: 23 Jan 2025 Accepted: 31 Mar 2025 ¹ lufei315@126.com, College of Air Traffic Management, Civil Aviation University of China, Tianjin, China



This work is licensed under a Creative Commons Attribution 4.0 International Licence.

Publisher: Faculty of Transport and Traffic Sciences, University of Zagreb

ABSTRACT

In this research, a comprehensive cross-route collision risk assessment model was developed with the aim of accurately determining the minimum safety interval for aircraft during cross-route flights. At the beginning of the study, the event tree analysis (ETA) method was adopted to meticulously break down the aircraft's flight process. Subsequently, a stochastic differential equation was established based on the route structure to precisely describe the aircraft's position change. The Monte Carlo method was then utilised to calculate the probability of conflicts. When the air traffic control officer's (ATCO) deployment malfunctions and is likely to trigger an alarm, the fault tree (FT) and dynamic event tree (DET) analysis methods were further employed. These two methods were used to calculate the failure probability of the warning system and the pilot's operation error probability respectively, thereby obtaining the failure probability during the warning adjustment process. The completed comprehensive assessment model has powerful functions and can efficiently simulate and accurately evaluate collision risks under different initial conditions.

KEYWORDS

collision risk; cross-routes; event tree analysis; alarming adjustment process; model of human cognitive reliability.

1. INTRODUCTION

In the field of air transport, collision accidents have always been a major safety concern. Although the incidence of collision accidents has decreased year by year due to technological advances, there are still problems that cannot be completely eliminated. Collisions can not only lead to casualties and environmental damage, but also cause significant economic losses [1]. The study of cross-en-route aircraft collision risk is essential to ensure the safe operation of aircraft and the effective planning of the route network. By analysing the risk of collision at different distances, combined with the value of the safety target level, the minimum safety interval can be determined, thus providing an important reference for en-route operation.

The commonly used methods for crash risk research include the REICH model, the EVENT model, the stochastic analysis model, the Monte Carlo simulation method, the position error model, event tree analysis (ETA), fault tree (FT) and other safety risk analysis methods, as well as a combination of the above models. In the 60s of the 20th century, the British scientist P. G. Reich proposed the Reich model for parallel routes over the North Atlantic and used it for the analysis of collision risks in the lateral, longitudinal and vertical directions, laying the theoretical basis for the safety assessment of flight intervals [2-4]. Brooker proposed the EVENT model based on the limitations of the Reich model, which focuses on the statistical distribution of planned position deviations, tends to overestimate the collision risk, is not easy to identify key parameters, and adds relevant influencing parameters such as collision detection systems [5]. The stochastic analysis model mainly uses stochastic processes to study the collision risk by solving partial differential equations, which can better simulate the real operating environment, but because the model is more complex, the application rate is

not high [6-7]. The Monte Carlo simulation method calculates the probability of a collision by simulating the actual operation of the aircraft in the air [8]. Applying Monte Carlo directly to simulation can lead to a lot of computational time, so scholars use mathematical methods to speed up the estimation process. In 2023, Figuet et al. proposed a new method that combines Monte Carlo simulations and extreme value theory to evaluate the probability of collisions in the air [9]. The positional error model emphasises the inherent accuracy error of ground and airborne navigation equipment and its time-varying characteristics, resulting in the impact of fluctuations in the actual distance between adjacent aircraft on the collision risk of two aircraft [10-13]. The safety risk analysis method can analyse the risk of air traffic collision by combining multiple factors such as the aircraft's own speed and position error with the error or failure of the technical system, human error and inaccurate estimation of weather conditions. It is also easy to combine with itself or other methods to extend the depth of crash risk studies. In 2012, Huang Baojun analysed the intervention process of ATCO on aircraft side yaw, and based on the study of the traditional EVENT collision risk model, he established a parallel route side collision risk assessment model that includes human cognitive reliability (HCR) [14]. In 2015, Zhang et al. proposed the concept of a mobility corridor to assess the associated collision risk by combining Monte Carlo simulations and dynamic event trees (DET), where Monte Carlo simulations are used to simulate the movement of aircraft within corridors and identify potential trajectories that may lead to collisions [15].

At present, most of the research on cross-en-route collision analysis is based on the REICH model and the EVENT model, and the application scenarios of parallel routes are extended by improving the collision risk template [16, 17] and optimising the model parameters [18]. In 2013, Han Songchen et al. used time interval as a variable to provide a collision risk analysis method for route intersections [19]. In 2019, Novak developed a minimum distance model to describe the impact of aircraft flight configuration changes on conflicts before and after crossing points [20]. In 2024, Wang et al. converted the distance interval into a time interval and established an aircraft collision detection model by shortening the time difference between aircraft crossing the intersection [21]. *Table 1* compares different cross-en-route collision risk models.

| | Model | Proposed workaround |
|---|--|--|
| 1 | Collision risk model at en-route intersections [19]. | Introduce time interval and aircraft speed variables |
| 2 | Minimum distance model [20]. | The impact of the change of route configuration before and after the crossing of the aircraft on the conflict |
| 3 | Aircraft collision detection model [21]. | Convert distance intervals into time intervals and shorten the time difference between aircraft crossing intersections |

Table 1 – Comparison of collision risk models of different cross-way routes

In summary, the research on cross-route collision risk mainly focuses on the mathematical modelling of route configuration, velocity and flow, which lacks the consideration of human factors, meteorological factors and system failures, and cannot be well integrated with the actual operation process.

In view of this, this paper intends to research the flight altitude layers within the height range concentrated between 8,000 m and 12,000 m during the cruising segment. The ETA method in safety risk analysis is adopted. The warning adjustment process is defined, and factors such as human factors and warning equipment during the flight are further considered to establish a collision risk assessment model for cross routes. Firstly, the ETA method is used to analyse the collision process of cross-route aircraft. Then, according to the characteristics of different risk factors, the following are discussed: (1) according to the fitting situation of aircraft positioning error and the specific configuration of the route, combined with the aircraft motion process, the stochastic differential equation is established to solve and determine the collision probability of the aircraft at the intersection. (2) Considering the failure of ATCO deployment to further develop the conflict into a warning, the failure probability of the airborne warning equipment and the error probability of the pilot's operation are calculated by combining the FT analysis method and the DET analysis method. Finally, the collision risk of cross-route aircraft is studied, and the collision risk change trend of each operation scenario under different initial distances in the warning adjustment process is considered, to provide a theoretical reference for aircraft operation and route planning. In this article, other dynamic changes (such as weather) other than human factors and warning equipment are not analysed and discussed. The Monte Carlo simulation process is not optimised, and it is only used as a simulation tool in this paper. The assumptions and models involved in this article are only applicable to the research in this article. If one considers applying them, they also need to take into account the actual situations related to the application scenarios.

2. COLLISION RISK ASSESSMENT MODEL

ETA is an effective tool for safety analysis, which can be used to evaluate and analyse various risk factors in aircraft operation scenarios, as shown in *Figure 1*. Based on the consequences of the accident, the probability of an aircraft collision can be calculated. Since the occurrence of a conflict will lead to a collision, the conflict event is regarded as the initial trigger point of the collision, which is mainly affected by the performance of the aircraft navigation surveillance system. In this context, the role of the ATCO is crucial, playing a central role in maintaining flight safety and preventing further risks. If the ATCO is negligent, misjudges or mishandles during the deployment process, it will lead to the failure of conflict resolution, which in turn will trigger the onboard warning device. For a more in-depth analysis of the post-warning process, it is defined as the warning reconciliation process. This phase mainly involves TA (traffic advisory) and RA (resolution advisory) of the alerting. The former mainly provides warning information. When the conflict develops to this stage, the pilot mainly relies on the RA decision consultation provided by the TCAS (traffic collision avoidance system) to directly operate the aircraft to ascend or descend to avoid the occurrence of collision, and this article mainly considers the RA stage. When the TCAS system fails, it cannot provide warning information, so it can only rely on the pilot's visual observation and his judgment and cognition of the intrusive aircraft to take appropriate actions to avoid the collision.

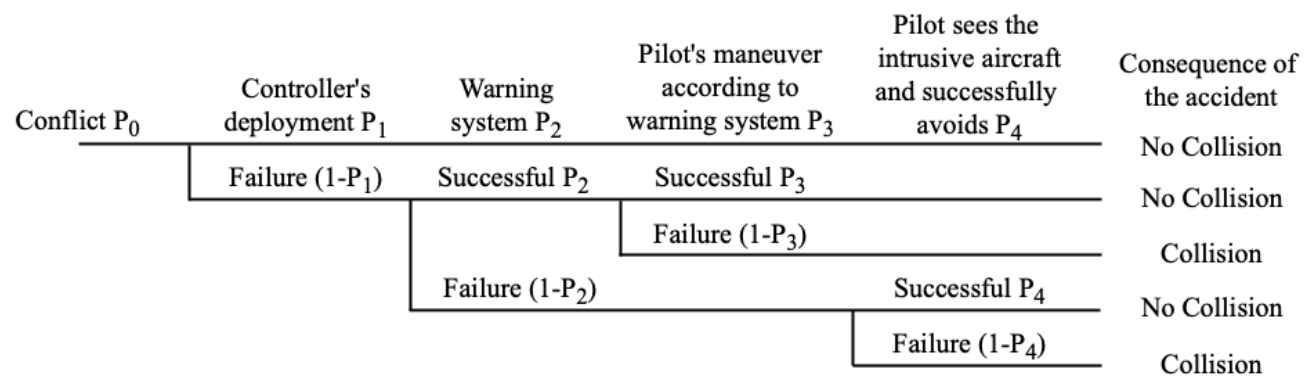


Figure 1 – Event tree analysis of the collision process

According to the above process, a cross-route aircraft collision process based on ETA method is established, which is divided into: P_0 representing the probability of conflict. P_1 indicates the probability of successful deployment of ATCOs' conflicts. P_2 indicates the reliability of the warning system. When the warning system is in good condition, the pilot will consult the probability of success (P_3) according to the decision provided by the warning system. P_4 indicates the probability that the pilot himself sees the intrusive aircraft and successfully avoids it, so the overall probability of warning adjustment failure is:

$$P_{failure} = P_2 \cdot \overline{P_3} + \overline{P_2} \cdot \overline{P} \tag{1}$$

Finally, by comprehensively considering the probability of conflict, the probability of warning occurrence caused by the failure of ATCO conflict deployment, and the probability of each potential accident outcome in the process of warning adjustment, the assessment model of cross-route collision risk is established as follows:

$$CR = 2NP \cdot P_0 \cdot \overline{P}_1 \cdot P_{failure} \tag{2}$$

where NP is the number of aircraft pairs analysed by the model. P_1 indicates the probability of successful deployment of ATCOs' conflicts. According to CAO:

$$P_1 = 1 - \prod_{i=1}^{4} (1 - CFP) \tag{3}$$

where *CFP* is the probability of cognitive failure. Other weighting factors of cognitive activity can be found in CAO.

3. PROBABILITY OF CONFLICT

The research object is divided into two directions, horizontal and vertical, that is, when the vertical direction overlaps, the operation characteristics in the horizontal direction are further considered. The expression for aircraft conflict is as follows:

$$P_0 = P_z(0) \times P_{xoy} \tag{4}$$

where $P_z(0)$ refers to the vertical overlap probability of layers of the same height. P_{xoy} represents the probability of collision between aircraft 1 and 2 in the horizontal direction.

3.1 Probability of vertical overlap at the same height layer

The probability of overlapping of layers at the same altitude depends mainly on the technical errors, i.e. the altimetry systematic error (ASE) and the flight technical error (FTE). By calculating these two errors, the overlap probability in the vertical direction can be approximated.

The altimeter system error is the difference between the altitude displayed on the altimeter display and the pressure height corresponding to the ambient pressure if the altimeter is set correctly, assuming that the altimeter barometric pressure is set correctly. In the process of altimetry, errors when measuring ambient air pressure or converting it into altitude readings are still a major source of ASE. But ASE still has some problems: in most cases, pilots, ground ATCOs and other aircraft are unclear of ASE, and the increased risk due to ASE cannot be operationally mitigated. ASE mainly depends on the aircraft type, and the overall ASE distribution is a combination of the ASE distribution of each aircraft monitoring classification, weighted according to the proportion of flights in that classification, and the specific formula is as follows:

$$f^{ASE}(a) = \sum_{i=1}^{n} \beta_i f_i^{ASE}(a), i = 1, ..., n$$
 (5)

where β_i is the weighting factor, which denotes the proportion of the flight time of Class I aircraft in the airspace to the total flight time of the entire airspace. Refer to the results of the analysis of altitude monitoring data in Europe (EUROCONTROL) to get the ASE fit for each aircraft monitoring classification, and in most cases, ASE conforms to the mixed distribution curve and the probability density formula is as follows:

$$f_i^{ASE}(z') = (1 - \alpha_i) \frac{1}{\sigma_{A_1} \sqrt{2\pi}} e^{-\frac{(z' - \mu_A)^2}{2\sigma_{A_1}^2}} + \alpha_i \frac{1}{2b_i} e^{\left|\frac{z' - \mu_A}{b_i}\right|}$$
(6)

where, $b_i = \sqrt{\frac{\sigma_{A_2}^2}{2}}$ and α_i indicate the systematic error of altitude measurement that obeys the proportion of a double exponential distribution. μ_A and σ_A the expectation and variance of the mixed distributions to which ASE obeys, respectively.

FTE can be approximated by the altitude hold error (AHE), which is the difference between the altitude of the C-mode transponder between the specified altitude and altitude layer, and its probability density obeys a double exponential distribution:

$$f^{AAD}(z'') = \frac{1}{2b} e^{\left|\frac{z'' - \mu_D}{b}\right|} \tag{7}$$

where μ_D and σ_D are the expectations and variances of the double exponential distribution to which AHE obeys, respectively, μ_D and σ_D are taken here for respectively and let $\mu_D = 0.035$, $\sigma_D = 39.8$.

The systematic error of altitude measurement and the deviation of the specified altitude of flight are independent of each other, and the probability density function of vertical overlap of aircraft 2 can be obtained according to the convolution formula:

$$f(z) = \int_{-\infty}^{\infty} f^{ASE}(z') f^{AAD}(z - z') dz'$$
(8)

where z = z' + z''.

Then, the calculation of the vertical conflict between two aircraft at the same height level is as follows:

$$P_z(0) = \int_{-\lambda_z}^{\lambda_z} \int_{-\infty}^{\infty} f(z_1 - z) f(z_1) dz_1 dz \tag{9}$$

where $\lambda_z = \sum_{i=1}^n \beta_i \lambda_{zi}$ represents the average height of the aircraft determined according to the proportion of each aircraft type in the airspace.

3.2 Probability of horizontal collisions

Near the intersection at the same altitude level, aircraft 1 flies at speed V_1 along a predetermined route $L_1L'_1$ and aircraft 2 flies at speed V_2 along a predetermined route $L_2L'_2$. The intersection angle of the route L_1 and the route L_2 before the intersection is θ_1 , and the intersection angle of the route L'_1 and the route L_2 after the intersection is θ_2 . Suppose the aircraft is sideways, longitudinal, the vertical positions are independent of each other, and the specific cross-route structure is shown in Figure 2.

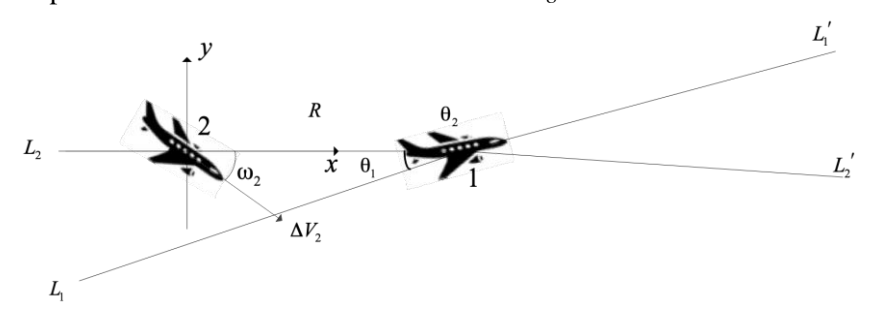


Figure 2 – Schematic diagram of aircraft relative motion

According to the characteristics of the cross-route configuration, the calculation of horizontal collision needs to be divided into two stages according to the aircraft movement process: (1) neither aircraft has passed the intersection point. (2) Aircraft 1 passes the intersection point, but aircraft 2 still moves towards the intersection point. The two-stage analysis process is the same, both take the moment when aircraft 1 is at the intersection point, and aircraft 2 is at the initial distance *R* as the starting state, and the motion state is deduced by time forward (stage 2) or backward (stage 1) respectively to calculate the corresponding conflict probability, the specific process is shown in *Figure 3*, and the second stage is selected to describe the motion process of the two aircraft.

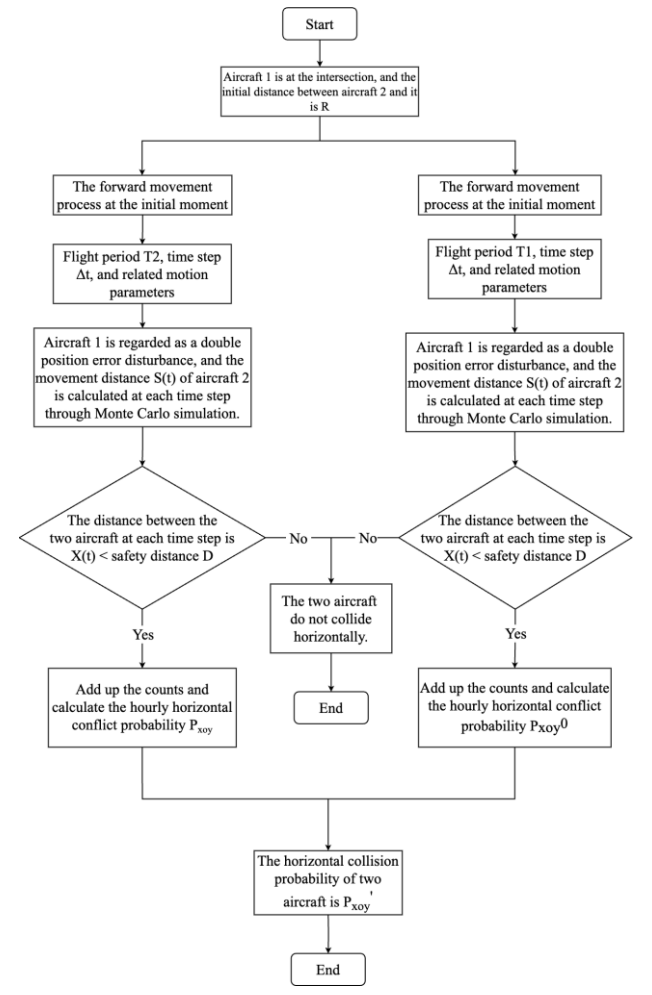


Figure 3 – Aircraft horizontal conflict probability calculation flowchart

At that $t = t_0$ time, the initial distance between the two aircraft is R, and aircraft 1 arrives at the intersection point first. The process of moving away from the intersection point is analysed, and the motion of aircraft 2 is regarded as deterministic motion, while aircraft 1 is perturbed with twice the position error. Assuming that aircraft 2 itself is the coordinate axis, and the heading is the x axis, and the plane Cartesian coordinate system is established accordingly, then the aircraft 2 flies to the intersection point in the direction of the relative velocity ΔV_2 and the angle ω_2 between its own predetermined route.

Well, at the moment t the kinematic model of aircraft 2 can be denoted as follows:

$$dS(t) = \Delta V_2 dt + \sum dB(t) \tag{10}$$

where the distance of motion of aircraft 2 at the initial moment is 0, i.e. $S(t_0) = 0$. B(t) is twice the position error of aircraft 1 at time t, and it follows a normal distribution $N(0,2\sigma^2)$, i.e. $B(t) \sim N(0,2\sigma^2)$. This can be calculated using the performance-based navigation definition, as follows:

$$\int_{-n}^{n} \frac{1}{\sqrt{2\pi}\sigma} e^{-\left(\frac{x^2}{2\sigma^2}\right)} dx = 0.95 \tag{11}$$

According to the definition of performance-based navigation, integrate the above formula; the solution can be obtained, $\sigma = 0.510213n$, where n represents the navigation accuracy value, and the en-route flight meets the RNAV2 navigation specification, that is, in 95% of the flight time, the aircraft position must meet the accuracy value requirements of the nominal track position within 2 nautical miles before and after.

The formula for calculating the relative velocity between two aircraft is as follows:

$$\Delta V_2 = \sqrt{(V_2 - V_1 \cos(\pi - \theta_2)^2 + (V_1 \sin(\pi - \theta_2))^2}$$
(12)

$$\omega_2 = \arctan \frac{V_1 \sin(\pi - \theta_2)}{V_2 - V_1 \cos(\pi) - \theta_2} \tag{13}$$

Then the distance between the two aircraft at the t moment can be determined by Equation 14. Derives:

$$X(t) = \sqrt{R^2 + S(t)^2 - 2RS(t)\cos\omega_2} \tag{14}$$

When X(t) < D, there would be a collision between the two aircraft, as D was the minimum safety interval specified. In the flight period T, as the step size Δt , the distance between two aircraft is simulated by Monte Carlo and compared with the minimum safety interval (D), and the number less than D is denoted as n, then the probability of horizontal collision per flight hour is:

$$P_{xoy} = \frac{n}{T/\Delta t}/T = \frac{n \times \Delta t}{T^2} \tag{15}$$

According to the above derivation process, the motion of the two aircraft in the first stage is described. Specifically, from the initial moment t_0 , the dynamic change process of the two aircraft gradually increasing with the backwards distance of time is simulated. Based on this, the probability of conflict P_{xoy}^0 in the first stage is calculated:

$$P_{xoy}^{0} = \frac{n \times \Delta t}{T_0^2} \tag{16}$$

where the time required for the first phase of the conflict is described as T_0 . Then, during the whole intersection movement, the probability of collision P'_{xoy} between the two aircraft in the horizontal direction is calculated as follows:

$$P'_{xoy} = P_{xoy}^{\ \ 0} + P_{xoy} \tag{17}$$

4. WARNING ADJUSTMENT FAILURE PROCESS

Warning adjustment is when the ATCO deployment fails, the distance between the two aircraft is further lost, when the time is less than the TCAS specified range, the warning information is issued, and then the pilot manoeuvres the aircraft out of danger according to the prompts, the flow chart is shown in *Figure 4*. The TCAS system communicates through transponders between aircraft. When two aircraft are too close together to collide, TCAS will generate a warning to inform the pilot to take measures to avoid the collision. There are two levels of alerting: conflict advisory and decision advisory.

- 1) TA: At this stage, the TCAS system detects a potential threat of collision and warns the pilot. This warning is suggestive and tells the pilot to be aware of the traffic around them.
- 2) RA: If the distance between the aircraft is further reduced, the TCAS system will issue a decision advisory, providing specific recommendations such as ascent or descent, and guiding the pilot to take specific manoeuvring measures to avoid collision to ensure the safe separation of the two aircraft. After receiving the RA, the pilot should follow the TCAS guidance to operate the aircraft and ensure that the recommendations provided by the system are followed to further avoid potential collisions. This autonomous decision-making capability makes the aircraft safer in areas with high air traffic, enabling timely and effective measures to be taken even without the guidance of an ATCO.

A key feature of TCAS alerting is that, after a conflict occurs, it relies on the time it takes for the aircraft to reach the point of closest approach (CPA) rather than the distance to decide when to issue an RA. This is important for the analysis of the warning adjustment process, using time as a variable to construct the flowchart shown in *Figure 4* to connect the warning system with the pilot's response actions.

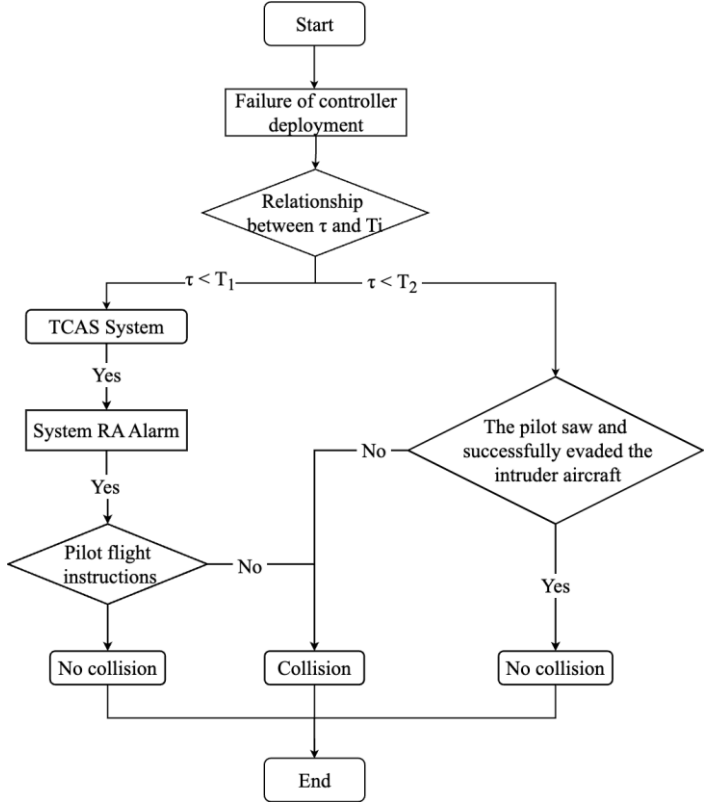


Figure 4 – Flowchart of warning adjustment process

Where τ represents the time remaining until the collision occurs, and the value is iteratively decreasing until the collision occurs or the danger is removed. T_1 , T_2 represent the time left before the pilot-in-command (PIC) visually invades the aircraft and the time left to collide when the RA warning is issued by TCAS and the TCAS warning fails.

According to the framework of the diagram above, the failure of the warning adjustment depends mainly on the reliability of the warning system as well as the pilot's operation. If the conflict is detected early, the pilot's operational time is long, the operational accuracy is high. Conversely, if the pilot's operating time is short, the probability of error will also increase. In this regard, the DET is used to add the time dimension to the state space of the standard event tree, and the response ability of pilots at different times is analysed through the HCR model. Here is how it works:

- 1) The failure probability of TCAS was calculated by FT analysis.
- 2) Construct two DETs based on whether the TCAS system works or not: DET1 (TCAS works normally) and DET2 (TCAS fails). According to different DETs, the influence of pilot operation on flight status and the corresponding probability are analysed over time, and the state transition matrix is established.
- 3) The probability of warning adjustment failure can be obtained by multiplying the probability of occurrence of the DET by the probability of collision in the corresponding transition matrix.

4.1 TCAS failure

The TCAS system consists of a directional antenna, a TCAS computer, an ATC/TCAS control panel, and is also affected by the associated equipment. In this regard, the TCAS failure is used as the top event G to analyse the reliability of the system, as shown in *Figure 5*.

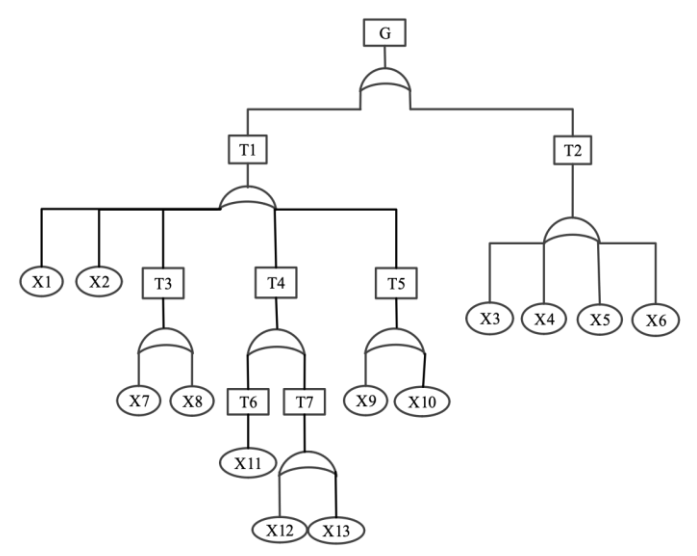


Figure 5 – TCAS fault tree

In Figure 5, G represents the top event of TCAS failure. T1 is the fault of the TCAS system itself. T2 is a TCAS-associated device failure. T3 is an antenna fault. T4 is a computer malfunction. T5 is an audio output failure. T6 is a false fault. T7 is a true fault. X1 is a TCAS display component failure. X2 is a transponder failure. X3 is an inertial navigation system failure. X4 is a radio altimeter fault. X5 is an electronic flight instrument system failure. X6 is a connection line fault. X7 is an antenna position fault. X8 is an antenna cable fault. X9 is a loudspeaker failure. X10 is an audio connection fault. X11 is a fault caused by radio interference. X12 is a hardware failure. X13 is a software failure (basic event failure rate Liu, through expert consultation, assuming that the failure rate as $\lambda = 10^{-5}/min$ and its lifetime obeys an exponential distribution, then the probability of component failure is $1 - e^{-\lambda t}$).

TCAS failures are all composed of OR gates, and each bottom event is independent of each other, and the probability of the top event is calculated as follows:

$$P_G = \overline{P_2} = 1 - \prod_{i=1}^{13} (1 - P(X_i)) \tag{18}$$

4.2 Pilot error

An individual analysing the state-time pairs may appear in the DET, and the state transition matrix is given. The main consideration is the probability of a pilot error in executing RA commands and visually identifying an aircraft and taking the correct action, which is based on the HCR model (SUN). The formula is as follows:

$$E = e^{-\left(\frac{t/\overline{T} - 0.7}{0.407}\right)^{1.2}} \tag{19}$$

where t represents the available time for selecting or performing an action. \overline{T} represents the average amount of time it takes to select or perform an action.

The RA alarming time of TCAS is related to the sensitivity level, and the higher the sensitivity level, the larger the protected airspace and the higher the warning threshold. In this paper, the altitude range is concentrated in 8,000 m-12,000 m, the corresponding sensitivity level is 7, and the RA value is 35 s [22]. While pilots receive RA, the average time to conflict resolution is 10 s (Brooker). Therefore, for DET1, a probability transition matrix can be established, as shown in *Table 2*. When it is in the state-time pair (A-35), the probability value is 1, and the derivation is calculated with it as the initial node. From the beginning, as the distance collision time decreases, the flight state of the aircraft is also constantly changing, until the collision occurs, and the failure probability of the pilot's execution of the warning information can be obtained (t = 1).

35s, $\overline{P_3} = 2.69 \times 10^{-5}$). (In the end, there are only 5 seconds left, and the pilot does not have enough time to adjust the altitude or visually escape after the TCAS alarm, so it directly changes to the collision state.)

| 64-4- | The time remaining until the collision t/s | | | | | |
|-------|--|-----------|-----------|-----------|-----------|--|
| State | 35 | 25 | 15 | 5 | 0 | |
| A | 1 | 0.018 000 | 0.000 198 | 1.19E-06 | | |
| В | | 0.981 960 | 0.999 716 | 0.999 892 | 0.999 892 | |
| С | | 3.96E-05 | 4.62E-05 | 2.07E-05 | | |
| D | | | 3.86E-05 | 8.09E-05 | 8.09E-05 | |
| And | | | 1.03E-06 | 4.98E-06 | 2.69E-05 | |

Table 2 – State-time transition probability table for DET1

The evolution of DET2 when the TCAS warning system fails is as follows: after the conflict occurs, the airborne collision avoidance system cannot be warned due to failure, and the conflict can only be resolved by the pilot's own vision. According to Meng, $\overline{T} = 19.5s$ is taken, depending on the relative speed of the two aircraft and the pilot's visual visibility in the air, i.e. $T_2 = \frac{8}{\Delta V}$. Then, the failure probability (P_{DET2}) of the DET can be obtained, i.e. $P_{DET2} = \overline{P_4}$.

Finally, combined with the formula, the probability value of alarming adjustment failure can be calculated. $P_{failure} = P_2 \times \overline{P_3} + \overline{P_2} \times \overline{P}$.

5. CROSS-EN-ROUTE COLLISION ANALYSIS

In this section, the ADS-B data of the Wuweitai intersection are obtained from the website of FlightAware, the world's largest flight dynamic tracking platform, and the obtained data are statistically analysed.

5.1 Longitudinal collision analysis

Through the statistics of aircraft types in the airspace near the intersection of Wuweitai, it is found that the aircraft with the highest flight frequency in this airspace are A320 and B738, respectively. In order to facilitate the calculation and follow-up research, only the aircraft with A320 and B738 models are selected as representatives, and other aircraft types are not considered. For the parameters of the A320 and B738 aircraft required in this paper, the weighted average values \overline{w} are calculated according to Equation 20

$$\overline{w}_{i} = \frac{\sum C_{i}w_{i}}{\sum w_{i}} = \frac{\beta_{i}w_{1} + \alpha_{i}w_{2} + \mu_{i1}w_{3} + \sigma_{i1}w_{4} + \sigma_{i2}w_{5} + \lambda_{z}w_{6}}{w_{1} + w_{2} + w_{3} + w_{4} + w_{5} + w_{6}}$$
(20)

where $\overline{w_i}$ is the weighted average of each parameter, C_i represents different parameters, and w_i is the corresponding weight value of each parameter. The collation and recording of each parameter's \overline{w} are recorded, and the results obtained are shown in *Table 3*.

| | Parameter | | | | | |
|--------|-----------|------------|---------|---------------|---------------|--|
| Models | eta_i | α_i | μ_i | σ_{i1} | σ_{i2} | |
| A320 | 0.4 | 0.199 8 | 37.5 | 43.570 41 | 48.192 18 | |
| B738 | 0.6 | 0.314 9 | 11.5 | 41.202 04 | 62.288 82 | |

Table 3 – ASE parameter values for aircraft types in the airspace near Wuweitai Station

According to the parameters obtained in *Table 3*, the probability density distribution function of the specific altitude measurement system error can be given, which is brought into *Equation 9*, respectively, and the vertical overlap probability between two aircraft at the same altitude layer is 0.00133.

5.2 Collision analysis of the same height layer

Next, it is necessary to further discuss the horizontal conflict between two aircraft at the same altitude level on a case-by-case basis. Aeronautical data of A320 and B738 aircraft on routes R474 and R339 were collected for analysis. There are two main scenarios to consider:

(1) Neither aircraft reached the intersection. At this time, the conflict needs to be considered that both aircraft fly to the intersection point until aircraft 1 first arrives at Wuweitai, as shown in Figure 6, where θ_1 indicates the angle between the two routes before crossing the intersection. By moving time forward to simulate the trajectory of two aircraft, the distance between the two aircraft increases as time goes backwards. According to its motion characteristics, the initial moment of aircraft 2 is regarded as the origin, and its own course is regarded as the x-axis. According to Equations 12 and 13, the previous aircraft is flying towards the origin at relative velocity ΔV_1 and angle w_1 at the intersection, and the calculation formulas are Equations 21 and 22.

$$\Delta V_1 = \sqrt{(V_2 - V_1 \cos \theta_1)^2 + (V_1 \sin \theta_1)^2} \tag{21}$$

$$\omega_1 = \pi - \arctan \frac{V_1 \sin \theta_1}{V_2 - V_1 \cos \theta_1} \tag{22}$$

Then, the spacing between the two aircraft at each time step is obtained by Monte Carlo simulation, and the number of spacing less than the value D is further counted, and then the horizontal collision probability $P_{xov}^{\ 0}$ of the two aircraft in the first stage is calculated.

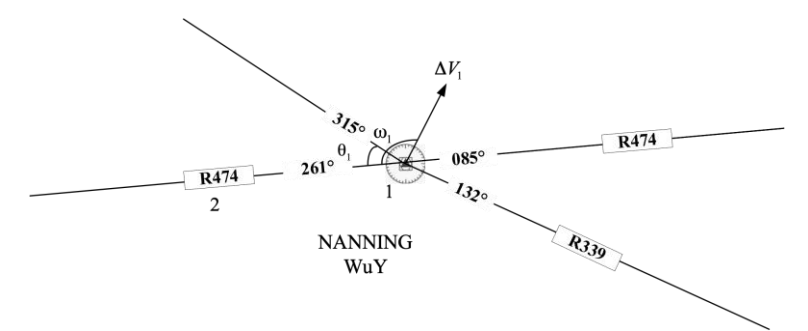


Figure 6 – Schematic diagram of the collision process between the two aircraft before reaching the intersection point

(2) The previous aircraft flies away from the intersection point, and the subsequent aircraft flies to the intersection point. This operation process is shown in Figure 7, where θ_2 shows that after the previous aircraft passes the intersection, the subsequent aircraft continues to drive towards the angle between the two routes at the intersection.

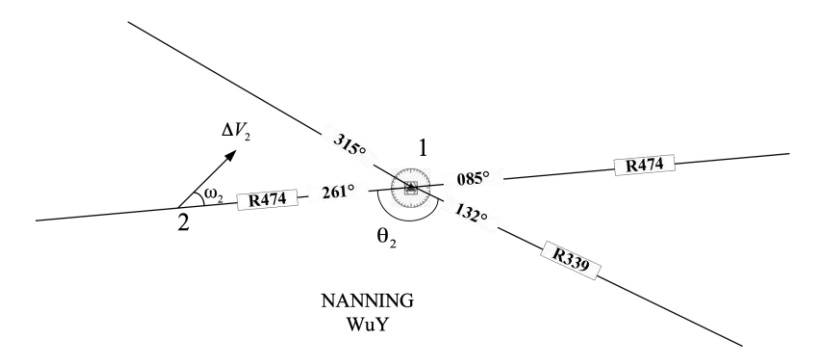


Figure 7 – Schematic diagram of the collision process between the two aircraft when the former aircraft is far away and the subsequent aircraft is heading towards the intersection

In this process, if the perturbation of position error is not considered, the formula for the change of distance between two aircraft over time is shown in *Equation 23*,

$$\sqrt{(R - V_2 t_2)^2 + (V_1 t_2)^2 - 2V_1 t_2 (R - V_2 t_2) con\theta_2} = d$$
(23)

The value of V_2 will be fixed as 800 km/h. Derivation,

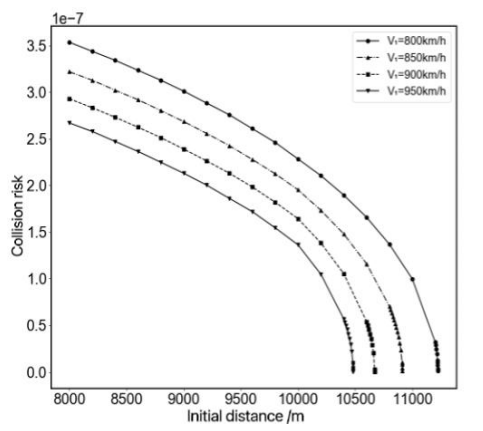
$$\frac{\partial(d)}{\partial t_2} = 2(V_2^2 + V_1^2 - 1.258V_1V_2)t_2 + (1.258V_1R - 2V_2R) \tag{24}$$

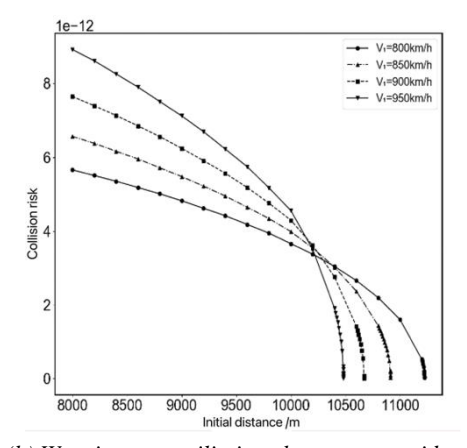
where $V_1 \in (503.2,950)$, the derivative value was less than 0 and then is greater than 0, which means that the distance between the two aircraft decreases and then increases. Based on this conclusion, the scenario shown in *Figure 7* is simulated. The position of aircraft 1 at the initial moment is regarded as the origin, and the relative velocity of the flight towards the origin at this time is ΔV_2 and its direction ω_2 can be determined by *Equations 12* and *13*. Then, through a Monte Carlo simulation, the distance between two aircraft at different time steps is calculated and compared. The probability of horizontal collision between the two aircraft in the second stage P_{XOV} can be obtained by *Equation 15*.

Finally, considering the above two cases, the horizontal collision probability of the two aircraft in the whole intersection operation process can be calculated from *Equation 17*.

5.3 Cross-en-route collision analysis

Based on CAO, the probability of ATCO deployment failure is calculated, $\overline{P_1} = 0.006882$, and the collision risk of the previous aircraft at different speeds is further analysed without considering the warning adjustment process, and its change trend is shown in *Figure 8(a)*. At the same time, considering the warning adjustment process, the collision risk model proposed in this paper is used for evaluation, and the final result is shown in *Figure 8(b)*.





(a) Warning reconciliation charts are not considered

(b) Warning reconciliation charts are considered

Figure 8 – Collision risk probability as a function of the initial distance

Figure 8(b) analyses the influence of the initial distance and the relative velocity of the two aircraft on the collision risk, visually shows the trend of collision risk after considering the warning adjustment process under different initial distance and forward speed, and especially investigates the influence of the warning adjustment process on the risk assessment. The results show that the risk of collision between two aircraft decreases significantly with the increase of the initial distance. Without considering the warning adjustment process, the higher the cruising speed of the front aircraft, the greater the speed difference between the two aircraft, and the lower the collision risk at the same initial distance, as shown in Figure 8(a). However, when considering the warning adjustment process, the trend of collision risk at different initial distances shows two different trends with the change of the preceding speed, as shown in Figure 8(b). In the case of a short initial distance, the motion state of the aircraft has reached the critical condition of conflict, and the danger is further aggravated, and the warning adjustment plays a decisive role. In this case, as the speed of the front aircraft increases, the relative speed difference between the two aircraft increases, and according to Equation 17, the probability of pilot error also increases, thus increasing the risk of collision. On the contrary, when the initial distance is long, the speed difference between the two aircraft maintains a safe operating distance, effectively reducing the risk of collision.

Finally, the model is used to analyse the aircraft collision risk at different route intersections near Wuweitai, and the average flight speed of the aircraft is about 800 km/h; the specific results can be seen in *Figure 9*. Under the safety interval requirements of the existing cross-sea routes, all intersections meet the safety target level. It is particularly noteworthy that the analysis results show that the greater the intersection angle before the

crossing of two aircraft, the greater the risk of collision with the same initial distance. In other words, given the level of a safety target (a θ_1 collision risk value of 1.5e-9 is selected as the safety target level, which is indicated by the red dotted line in the figure), the corresponding initial distance increases as the intersection angle increases. This phenomenon is mainly related to the relative motion characteristics of the two aircraft: the larger the intersection angle, the higher the relative velocity, which means that the less time it takes for the aircraft to shorten the distance between them. In order to ensure sufficient time to detect and evade potential intrusive aircraft, it is necessary to increase the initial distance between them. At the same time, higher relative speeds can make flight control more complex, increasing the risk of pilot error. In this regard, in order to reduce the probability of collision, it is particularly important to increase the initial distance between two aircraft.

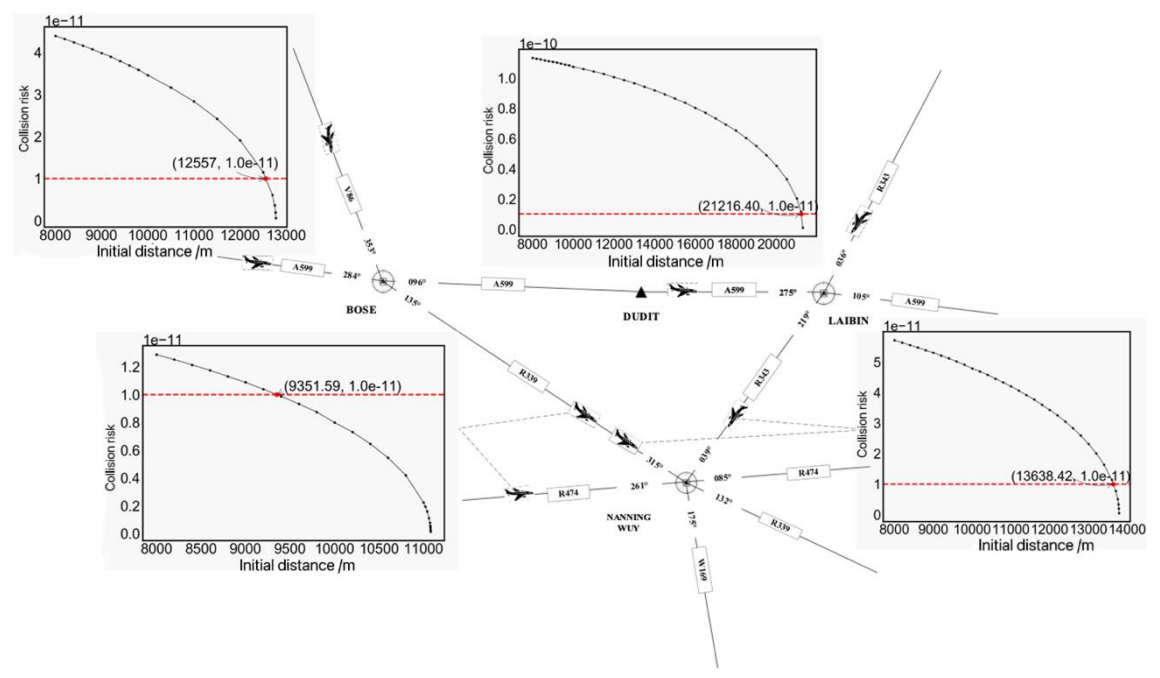


Figure 9 – Collision risk probability as a function of the initial distance

6. CONCLUSION

The ETA method is used as the core tool, and the three stages of "conflict occurrence", "ATCO monitoring failure" and "alarming adjustment process failure" are considered. A comprehensive assessment model for cross-en-route collision risk was constructed. This paper focuses on the analysis of the mechanism of "conflict occurrence" and "alarming adjustment process failure", and the following conclusions are drawn.

For calculating the collision probability at en-route intersections, constructing the kinematic equation should account for the transformation of the intersection-route configuration. It needs to be discussed in stages, taking into account the influence of different en-route configurations on the operational safety of the whole intersection, and enhancing the accuracy and applicability of the conflict simulation results.

After considering the warning adjustment process, the influence of the relative velocity of the aircraft at different initial distances shows obvious duality. When the initial distance is short, a greater relative velocity between two aircraft increases the post-collision danger level and the requirements for pilot operation, leading to a higher collision probability. Conversely, when the initial distance between the two aircraft is larger, the greater the relative velocity, the greater the corresponding distance between the two aircraft, and the higher the safety.

Under the premise of a fixed initial distance, the collision risk between intersections under different flight path configurations shows significant differences. In other words, en-route intersections with large crossing angles, especially obtuse angles, need to be set at a longer initial distance in order to achieve a preset level of safety objectives, after taking into account the alarming adjustment process. This finding provides a key scientific basis for the formulation of cross-route planning strategies and has practical significance for improving the safety of air traffic management.

ACKNOWLEDGEMENTS

Fei Lu gratefully acknowledges the contributions of Yuxuan He (heyuxuan9826@gmail.com) and Jian Zhang (zhangjian@cauc.edu.cn), both of the Civil Aviation University of China, College of Air Traffic Management. Their collaboration and insights were vital to the completion of this paper. National Natural Science Foundation General Project (52272356), Central University Basic Operating Expenses (3122022101).

REFERENCES

- [1] Boeing. Statistical summary of commercial jet airplane accidents worldwide operations 1959-2020. United States: Boeing, 2021.
- [2] Reich PG. Analysis of long-range air traffic systems: Separation standards I. *Journal of Navigation*. 1966;19(1):88-98. DOI: 10.1017/S037346330004056X.
- [3] Reich PG. Analysis of long-range air traffic systems: Separation standards II. *Journal of Navigation*. 1966;19(2):169-186. DOI: 10.1017/S0373463300047196.
- [4] Reich PG. Analysis of long-range air traffic systems: Separation standards III. *Journal of Navigation*. 1966;19(3):331-347. DOI:10.1017/S0373463300047445.
- [5] Brooker P. Lateral collision risk in air traffic track systems: a 'post-reich' event model. *Journal of Navigation*. 2003;56(3):399-409. DOI: 10.1017/S0373463303002455.
- [6] Bakker GJ, Blom HAP. Air traffic collision risk modelling. *Proceedings of 32nd IEEE Conference on Decision and Control.San Antonio,TX,USA*:IEEE.1993;1464-1469. DOI: 10.1109/CDC.1993.325430.
- [7] Blom HAP, et al. Collision risk modeling of air traffic. 2003. *European Control Conference (ECC)*. Cambridge,UK:IEEE. 2003;2236-41. DOI: 10.23919/ECC.2003.7085299.
- [8] Wang C, Li YK, Li HY. Collision risk analysis of parallel runway approach based on Monte Carlo. *Journal of Safety and Environment*. 2023;23(03):659-66. DOI:10.13637/j.issn.1009-6094.2021.1741.
- [9] Figuet B, et al. Data-driven mid-air collision risk modelling using extreme-value theory. *Aerospace Science and Technology*. 2023;142:108646. Doi: 10.1016/j.ast.2023.108646.
- [10] Zhang ZN, Shen JW, Liu JM. Lateral collision risk model based on CNS position error. *Journal of Traffic and Transportation Engineering*. 2009;9(06):110-3. DOI:1 0.19818/j.cnki.1671-1637.2009.06.021.
- [11] Zhang ZN, Liu JM, Wang LL. Assessment of longitudinal collision risk on parallel routes based on communication, navigation, and surveillance performances. *Journal of Southwest Jiaotong University*. 2009;44(06):918-925. DOI: 10.3969/j.cnki.issn10258-2724.2009.06.021
- [12] Lu F, et al. Assessment of lateral collision risk in closed spaced parallel runways paired approach. *China Safety Science Journal*. 2016;26(11):87-92. DOI: 10.16265/j.cnki.issn1003-3033.2016.11.016.
- [13] Lu F, Chen HN. Longitudinal collision risk of CSPRs paired approach under funny PID control. *China Safety Science Journal*. 2023;33(11):97-104. DOI: 10.16265/j.cnki.issn1003-3033.2023.11.0895.
- [14] Huang BJ. Lateral collision risk model on parallel routes based on communication, navigation and surveillance performances. *Journal of Southwest Jiaotong University*. 2012;47(06):1075-1080+1091. DOI: 10.3969/j.issn.0258-2724.2012.06.026.
- [15] Zhang Y, Shortle J, Sherry L. Methodology for collision risk assessment of an airspace flow corridor concept. *Reliability Engineering & System Safety*. 2015;142:444-455. DOI: 10.1016/j.ress.2015.05.015.
- [16] Cao XW, Zhang ZN. Cross route collision risk assessment based on improved Event model. *Journal of Civil Aviation University of China*. 2015;33(03):1-4.
- [17] Zhang L. Collision risk of crossing airlines at the same altitude based on REICH model. *Journal of Shenzhen University Science & Engineering*, 2020;37(2). DOI: 10.3724 /SP.J.1249.2020.02136.
- [18] Meng X, Zhang P, Wang Y. Aircraft collision risk assessment at intersecting air routes. *Journal of Beihang University of Aeronautics and Astronautics*. 2010;36(9):1021-5. DOI: 10.13700/j.bh.1001-5965.2010.09.004.
- [19] Songchen H, Yuling Q, Fanrong S, Xinping Z. Collision risk model around intersection of airways. *Journal of Southwest Jiaotong University*. 2013;26(2):383-9. DOI: 10.3969/j.issn.0258-2724.2013.02.029.
- [20] Novak A, Havel K, Adamko P. Number of conflicts at the route intersection—minimum distance model. *Aviation*. 2019;23(1):1-6. DOI: 10.3846/aviation.2019.9746.
- [21] Wang LL, Liu XY.Research on cross-flight flow pre-conflict resolution based on auto-rerouting. *Journal of Southwest Jiaotong University*. 2024;1-9.

- [22] Federal Aviation Administration. *Introduction to TCAS II Version 7.1*. United States. Federal Aviation Admianistration, 2011.
- [23] Sun RS, Chen YF. Application of CREAM predictive method in conflict resolution by air traffic controllers. In Proceedings of 2010 (Shenyang) *International Colloquium on Safety Science and Technology* 2010.
- [24] EUROCONTROL, THE EUR RVSM safety monitoring report. Brussels: EUROCONTROL, 2004.
- [25] Shortle J, Sherry L, Yousefi A, Xie R. Safety and sensitivity analysis of the advanced airspace concept for NextGen. *In2012 Integrated Communications, Navigation and Surveillance Conference 2012 Apr 24 (pp. 02-1).* IEEE. DOI: 10.1109/ICNSurv.2012.6218434.
- [26] Sun R, et al. A method of analysis integrating HCR and ETA modeling for determining risks associated with inadequate flight separation events. *Journal of Aviation Technology and Engineering*. 2011;1(1):5. DOI: 10.5703/1288284314632.
- [27] Brooker P. STCA, TCAS, airproxes and collision risk. *The Journal of Navigation*. 2005;58(3):389-404. DOI: 10.1017/S0373463305003334.